

TURBULENCE MODELING S AND APPLICATIONS TO AEROSPIKE PLUG NOZZLE

Manolo Pires

***Instituto Militar de Engenharia-Pça Gen.Tibúrcio s/n Praia Vermelha –Rio de Janeiro-
Brazil**

Keywords: *Turbulence, Aerospike, Reynold Stress*

Abstract

The increasing demand for higher performance in aerospace propulsion promotes the development of nozzles with higher performance which is basically achieved in plug nozzles. Thus, a renewed interest into plug nozzles has arised for the possible replacement of standard nozzles used for the propulsion systems of space vehicles. Although a more complex flow field develops on plug nozzles, the potential thrust and structural gains are attractive as the propulsive flow is free to adapt to the external stream. The prediction of complex high speed flow fields in fluid dynamics often involves the modeling of turbulence. In this paper, a research on recent turbulence models taking into account the physical Reynolds stresses is proposed. Efficient state of the art numerical tools have been developed and are used for the simulation of increasingly complex flow fields. Flow fields varying plug nozzles are simulated for twodimensional, axisymmetric configurations. Although very promising, the recent set of anisotropic models suffer from the same shortcomings than standard models because of the basic assumptions made in the Navier-Stokes equations.

1. Introduction

The plug nozzle concept has been proposed in the 60s to limit thrust losses due to jet over-expansion and to confer to the nozzle some self-adaptation capabilities without having to modify its shape. In this arrangement, the supersonic expansion is realized along a center body - or plug - is place of an external contour, as in a classical nozzle. This idea has been reconsidered to equip hypersonic vehicles or space launchers having to fly in conditions strongly out of adaptation. Such nozzles can be

linear or axisymmetric. In the later case, the flow coming from the engine can be ejected either through an annular throat or a series of small nozzles surrounding the plug.

Turbulence is a state of a physical system with many interacting degrees of freedom deviated far from equilibrium. This state is irregular both in time and in space. Turbulence can be maintained by some external influence or it can be decaying turbulence on the way of relaxation to equilibrium. As the term suggests, it first appeared in fluid mechanics and was later generalized for far-from-equilibrium states in solids and plasma. One of the challenging area of modeling in fluid dynamics is the turbulence modeling and the understanding of complex flow fields, such flows develop behind bluff bodies and they are characterized by large separated flows. A special case of such base flows is for a propulsion system composed configuration is called a plug-nozzle.

In the configuration plug-nozzle three classes of "unconventional" propulsion devices can be distinguished [1]. First, there is the expansion-deflection nozzle, however it has poor performance and presents high heating rates at walls. Second, one has the single throated toroidal and linear aerospikes; although good performance can be achieved, very high wall heating rates are present due to the throat thinness. Finally, one has the clustered or multi-nozzles toroidal and linear aerospike presenting low wall heating rates and good aerodynamic performance. From the advent of rockets, launchers and space vehicles, the base principle used for the propulsion system is the classical De-Laval shaped nozzle (or alternatively simpler conical nozzles). This family of nozzles can be seen as a simple duct with a converging

and diverging section. The flow is accelerated up to sonic speeds at the nozzle throat, it is then expanded in the diverging section because of the increased cross sectional area. Moreover, the flow field developing in such devices is easy to predict. However, several problems occur with such devices mainly because contoured/conical nozzles are not adaptable to the outside pressure and work optimally for one set of conditions. In space launchers, the nozzle design is made as to have optimal thrust for the trajectory part in the upper atmosphere where the ambient pressure is low and as to avoid flow separation at sea level; this is simply because introduction most of the flight time is spent in these conditions and optimizing thrust for high altitudes yields the highest specific impulse (I_{SP}). The I_{SP} is the most important criteria for a propulsion system as it directly relates to the payload that can be sent. Flow separation at sea-level and good performance at high altitude are not compatible in terms of design and to limit this problem one uses very high pressure combustion chamber pressures. When working at off-design conditions and especially for high ambient pressures, that is for take-off and low-altitude conditions, severe problems arise. Because of the external pressure, the flow expanding in the diverging section is pushed toward the center-line of the nozzle; this corresponds to an over-expanding jet flow Figure 1. Because of this over-expansion, two phenomena appear : – first a Mach disk is created at the nozzle outlet (inducing losses and thus less thrust) ; – then, inside the nozzle flow separation takes place. This creates high loads on the nozzle side walls and it is the source of very large vibrations which may result in catastrophic structural failures. It can be noted that the flow separation can be asymmetric even in axisymmetric configurations and thus one must pay large attention to the flow field which becomes complex. In this paper characteristics of plug nozzle flow fields are discussed based on the results of numerical simulations. At very high

altitudes, near vacuum conditions, the jet exiting out of the contoured nozzle is pulled away from the nozzle center line, it is an under-expanding jet Figure 1. Only for the design conditions, one will obtain a jet parallel to the nozzle exit walls and optimum thrust will be generated. In this operating conditions, the nozzle flow is said to be adapted. This analysis for a nozzle without taking into account the jet interaction which occurs when multiple nozzles are present highlights the short-comings of the contoured nozzles which mainly result from the inability of the flow to adapt to the external pressure. Starting from the late fifties until the early seventies, a new design for a propulsion system has been explored. Of interest are the first publications on this concept from [2] at the von Karman Institute. Large experimental work has then been conducted by General Electric; it was pursued by Rocketdyne [3]. This propulsion device is based on a series of small thrusters exhausting on a ramp where the flow is expanded and gains momentum. As no external ramp is present, the flow is free to be under or over-expanded depending on the external pressure. The jet flow can adapt itself to external conditions and instead of having a solid outer wall on which the flow expands, one has an aerodynamic wall. The great advantage of this system is that an optimal thrust can be produced throughout the trajectory of the rocket or space vehicles. Also, as the thrust is introduced in a distributed manner, a better launcher propulsion system integration can be done. This integration is also facilitated by the shorter length at similar expansion ratio. The long spike of the configuration and the aerodynamic wall gave the name of "aero-spike". Aerospikes are actually not feasible from a thermal and structural view point and the spike is cut, this forms the "plug nozzle"; the names aerospike and plug nozzle are often interchanged.

TURBULENCE MODELING S AND APPLICATIONS TO AEROSPIKE PLUG NOZZLE

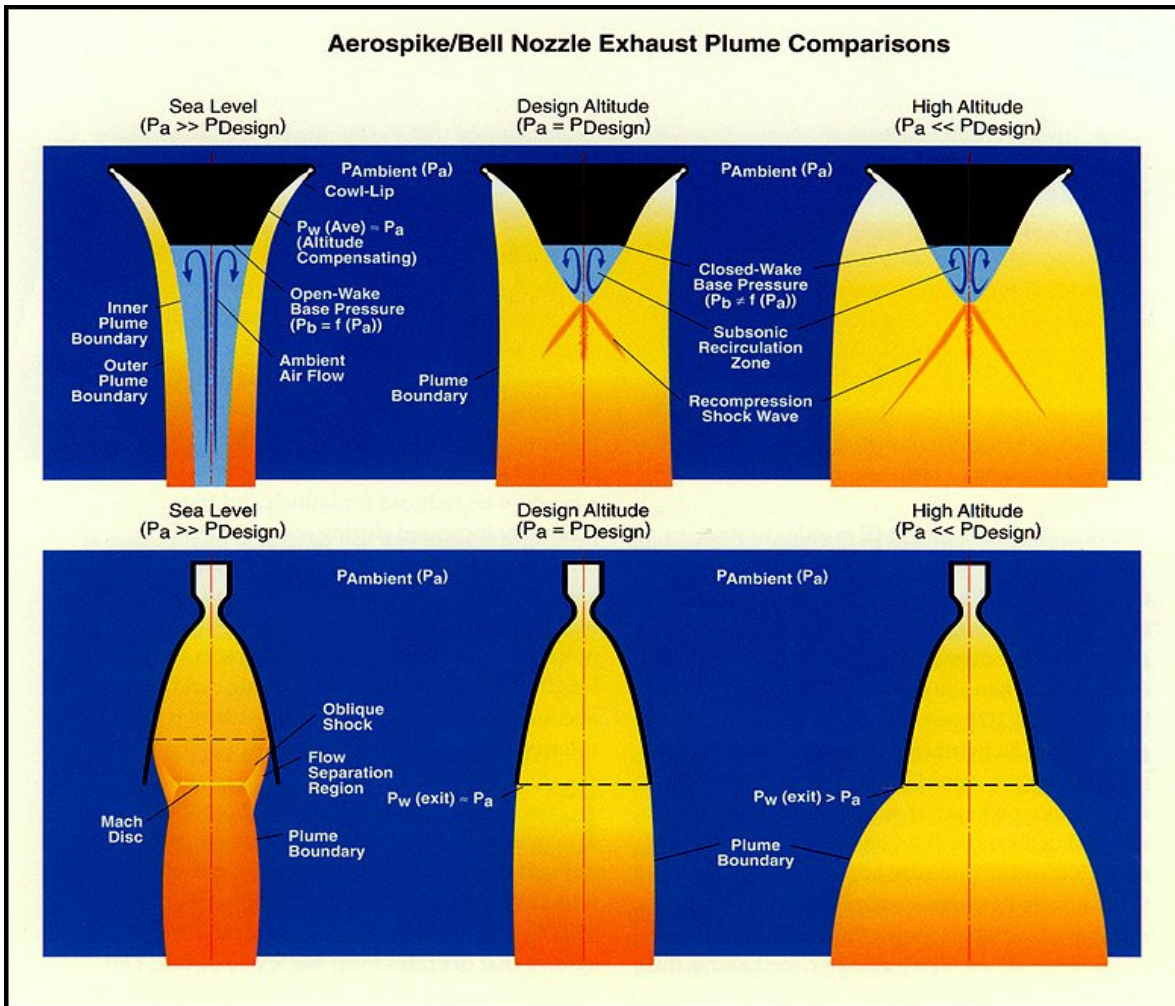


Figure 1. Plug Nozzles /Bell Nozzle Exhaust Plume Comparisons Nozzles- Over Expanded, adapted under Expanded Jet Flow for increase Altitude by R.A. O'Leary and J. E. Beck,Rocketdyne

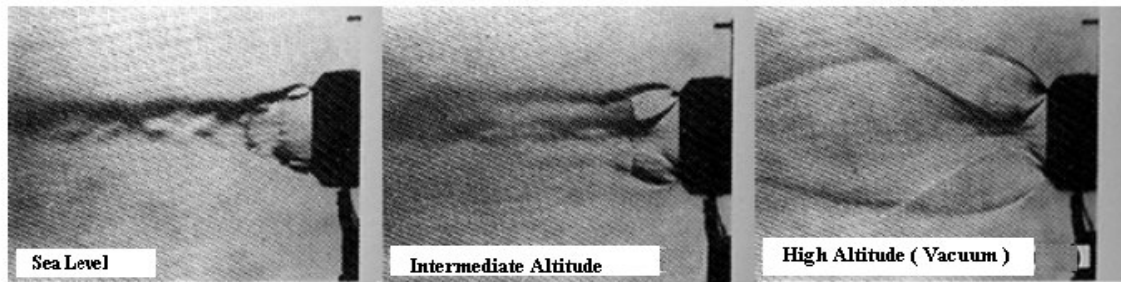
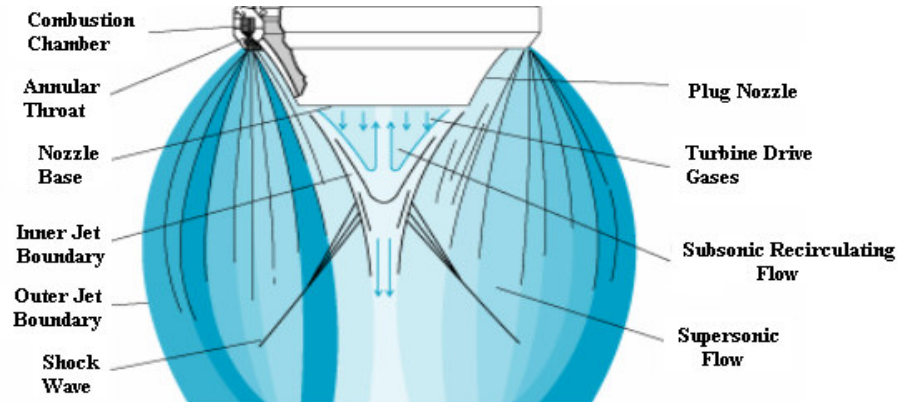
2. Turbulence Modeling

Currently, the feasible way to simulate complex, turbulent, high-Reynolds number flow using CFD techniques is through turbulence modeling methods. In this way, the many complex turbulent flow features and disparate length scales are replaced by a few physically based modeling equations. The modeling equations range from simple algebraic models, to complex second-order closure methods. The primary goal of all the models is to accurately represent Reynolds stress, representing the stress caused by the fluctuating or turbulent parts of the fluid flow. Turbulence is by nature strongly non-linear, that is why methods based on statistical approaches have a limited success. The most complete way of predicting turbulence is to

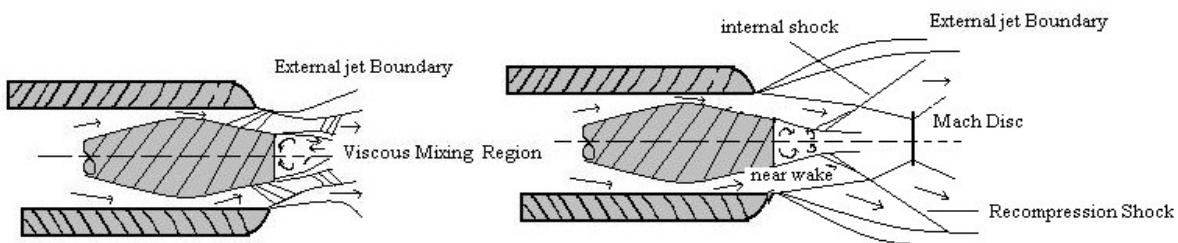
solve for the full Navier- Stokes equations directly. In this method, called Direct Numerical Simulation (DNS), one solves for the entire time and length scales. However, this method is not usable except for flows with low Reynolds numbers as the space resolution and computational time is very large. A simpler approach consist in only solving for the large scale structures, this is called Large Eddy Simulation (LES). The effect of the smallest turbulence scales is modeled using sub-grid models. The separation of the large and small scales structures is done through a filtering operation and thus one solves for the filtered Navier-Stokes equations. These two methods solve for the complete three-dimensional unsteady flow and require large computational

times because all the scales of motions are solved. Also, the initial boundary conditions for DNS or LES is a difficult matter and often requires to address the entire problem. Reducing further the spectrum of time and length scales, one arrives to second order closure methods which represent the highest closure level for practical applications especially for high

Reynolds number and high speed flows. These methods, where all the Reynolds stresses are solved, have shown good results since they account for history and non-local effects; however they are still costly and numerical difficulties arise because of the absence of turbulent viscosity. A renewed interest has been



Altitude Effect Flow Test Model; Schlieren Photographs the Aerospike Nozzle (Courtesy Rockwell International, Rockdyne Division)



Low Altitude Operation " Open Wake"

High Altitude Operation " Closed Wake"

Figure 2 Truncated Plug Nozzles – Low and High Altitudes Operations

recently paid to second order closure methods as they can be used to derive a new generation of point closure family. Finally, one can consider single point closure methods which are based on

more general and more accurate two equation type models which formally belong to the one a modeling of the Reynolds stress tensor in the

Reynolds Average Navier-Stokes equations (RANS) [1].

2.1 K-ε Turbulence Model

A Reynolds-averaged approach is employed for solving the turbulence field in the Navier-Stokes equations. After reviewing the various methods for the numerical simulation of turbulence, the averaged Navier-Stokes equations and the closure problem are presented. The turbulence modeling through algebraic models and then through transport equations models are then considered. Among the possible choices, the three most popular one are : ε the dissipation per unit mass, ω the specific dissipation rate (ω=ε/k), τ the reciprocal of ω.

The *K-ε model* is the most popular turbulence model, it exists under many variants. The latter formulation from [4] is one of the most elegant and it is briefly proposed here.

The two transport equations write :

$$\begin{aligned} \frac{\partial \rho k}{\partial t} + \frac{\partial}{\partial x_j} \rho u_j k &= \tau_{ij} S_{ij} - \rho \varepsilon + \frac{\partial}{\partial x_j} \left[\left(\mu + \frac{\mu_t}{\sigma_k} \right) \frac{\partial k}{\partial x_j} \right] \\ \frac{\partial \rho \varepsilon}{\partial t} + \frac{\partial}{\partial x_j} \rho u_j \varepsilon &= C_{\varepsilon 1} \frac{\varepsilon}{k} \tau_{ij} S_{ij} - C_{\varepsilon 2} \rho^2 \frac{\varepsilon}{k} + \\ &+ \frac{\partial}{\partial x_j} \left[\left(\mu + \frac{\mu_t}{\sigma_\varepsilon} \right) \frac{\partial \varepsilon}{\partial x_j} \right] \end{aligned} \quad (1)$$

One may recognize the Eulerian derivative on the left hand side. On the right hand side, one has the production term, the destruction term and the diffusion term. The eddy viscosity definition is :

$$\mu_t = \rho C_\mu k^2 / \varepsilon \quad (2)$$

The closure coefficient for this model are:

$$C_{\varepsilon 1} = 1,44, C_{\varepsilon 2} = 1,92, C_\mu = 0,09, \sigma_k = 1,0, \sigma_\varepsilon = 1,3$$

2.2 k – ω Turbulence Model

It is often thought that the *k-ω model* has been the first two-equation turbulence model.

However, even before Prandtl one equation model [5], proposed the foundations for a two equation model based on the transport of the turbulence kinetic energy and the specific dissipation rate. This choice of variables has been investigated by many other researchers and especially [6]. The formulation of the k and ω variables is given by:

$$\begin{aligned} \frac{\partial \rho k}{\partial t} + \frac{\partial}{\partial x_j} \rho u_j k &= \tau_{ij} S_{ij} - \rho \beta^* k \omega \\ &+ \frac{\partial}{\partial x_j} \left[\left(\mu + \sigma^* \mu_t \right) \frac{\partial k}{\partial x_j} \right] \\ \frac{\partial \rho \omega}{\partial t} + \frac{\partial}{\partial x_j} \rho u_j \omega &= \alpha \frac{\omega}{k} \tau_{ij} S_{ij} - \beta \rho \omega^2 + \\ &+ \frac{\partial}{\partial x_j} \left[\left(\mu + \sigma \mu_t \right) \frac{\partial \omega}{\partial x_j} \right] \end{aligned} \quad (3)$$

The eddy viscosity definition is:

$$\mu_t = \rho k / \omega \quad (4)$$

The closure coefficient for this model are:

$$\alpha = 5/9, \beta = 3/40, \beta^* = 9/100, \sigma = 1/2, \sigma^* = 1/2$$

When comparing the *k-ε* and the *k-ω models*, it appears that they both have pros and cons. The *k-ε model* better predicts the flow properties for free shear flows than *the k-ω model*, however the opposite it true for wall bounded shear flows (i.e. boundary layers).

2.3 Two layer BSL (baseline model) and SST (Shear Stress transport) turbulence models

These models which have been developed by [7] are based on a blending between the k-ε and the k-ω turbulence models. The idea is to use the desirable properties of both models, namely that outside boundary layers, the k-ε behaves well with a low dependency on free stream conditions, and near walls the model reverts to the k-ω formulation. This blending

makes the BSL (baseline model) wall dependent.

The first step in deriving this model is to reformulate the k-ε model with a variable change from ε to ω. This formulation gives rise to an extra term, a cross-diffusion term, in the dissipation equation. This has just been discussed in the presentation of the latest k-ω from [6]

$$\begin{aligned} \frac{\partial \rho k}{\partial t} + \frac{\partial}{\partial x_j} \left[\rho u_j k - (\mu + \sigma_k \mu_t) \frac{\partial k}{\partial x_j} \right] &= \tau_{ij} S_{ij} - \rho \beta^* k \omega \\ \frac{\partial \rho \omega}{\partial t} + \frac{\partial}{\partial x_j} \left[\rho u_j \omega - (\mu + \sigma_\omega \mu_t) \frac{\partial \omega}{\partial x_j} \right] &= P_\omega - \beta \rho \omega^2 + \\ + 2(1 - F_1) \frac{\rho \sigma_{\omega 2}}{\omega} \frac{\partial k}{\partial x_j} \frac{\partial \omega}{\partial x_j} & \end{aligned} \quad (5)$$

The production term in the dissipation equation is :

$$P_{\omega = \gamma \mu} = \frac{\rho}{\mu_t} \tau_{ij} S_{ij} \quad (6)$$

The blending function F1 which is the core of the BSL model formulated by [9] is :

$$F_1 = \tanh \left[\left(\min \left(\max \left(\frac{\sqrt{k}}{0,09 \omega y}, \frac{500 \mu}{\rho y^2 \omega} \right); \left(\frac{4 \rho \omega_2 k}{CD y^2} \right) \right) \right)^4 \right] \quad (7)$$

The cross-diffusion term is :

$$CD = \max \left[\frac{2 \rho \sigma_{\omega 2}}{\omega} \frac{\partial k}{\partial x_j} \frac{\partial \omega}{\partial x_j}; 10^{-20} \right] \quad (8)$$

The F1 function will take a value close to 1 near walls and close to 0 elsewhere. To close this turbulence model, one needs to give the appropriate model constant. These constants are found using the same blending function F1, they write:

$$\varphi = F_1 \varphi_\omega + (1 - F_1) \varphi_\varepsilon \quad (9)$$

for $\varphi = (\sigma_k, \sigma_\omega, \beta, \gamma)$. Each coefficient is taken from their respective original formulation as :

$$\begin{aligned} \sigma_{k\varepsilon} &= 0.85, \quad \sigma_{\omega\varepsilon} = 0,5, \quad \beta_\varepsilon = 0.075, \quad \gamma_\varepsilon = 0.553 \\ \sigma_{k\omega} &= 1.00, \quad \beta_\omega = 0.075, \quad \gamma_\omega = 0.553 \end{aligned}$$

Together with the turbulence viscosity, or eddy viscosity, which has the same formulation as in the k-ε model, one obtains the BSL turbulence model. For the derivation of the SST (shear stress transport) model, followed the same approach with the addition of a limitation on the eddy viscosity for rapidly strained flows. The model is thus similar to the BSL formulation excepted that the eddy viscosity is now :

$$\mu_t = \frac{\rho k / \omega}{\max(1; \Omega F_2 / (a_1 \omega))} \quad (10)$$

V is the vorticity. The F2 function which is wall dependent is similar to the expression given for the F1 function, it is :

$$F_2 = \tanh \left[\max \left(\frac{2\sqrt{k}}{0,09 \omega y}, \frac{500 \mu}{\rho y^2 \omega} \right) \right]^2 \quad (11)$$

This correction guarantees that the turbulent shear-stress does not respond instantaneously to changes in strain in boundary layer flows.

3. Grid Generation

In this paper, the computational work presented is based on a structured grid generator commercial software such as GridPro Software actively developed at R.Tech: adapted by the present author for axisymmetric plug nozzle. The computational structured grids for discretising the flow on the plug nozzle are shown in Figure 3, set of 6 domains are selected with a fine grid spacing near all walls.

4. Numerical methods

To perform the numerical simulation of turbulent flows, a Fortran 77 Program "Plug Nozzle" code is development, by author and based in the software developed at R.Tech Mistral. Solutions of the Euler, Navier-Stokes and RANS equations. State-of-the-art numerical techniques are employed such as dual time stepping (for truly second order time accurate computations), explicit/implicit (GMRES) methods and low speed preconditioning. Wide range of turbulence models. This Program, Plug Nozzle, is extended for the modeling of

TURBULENCE MODELING S AND APPLICATIONS TO AEROSPIKE PLUG NOZZLE

turbulence; it solves for the two-dimensional and axisymmetric flow fields. The turbulence models which have been used to this configuration, namely, the $k-\omega$ and the two layer blended models (BSL and SST) are used

and the effect of compressibility corrections is investigated. The anisotropic (quadratic and cubic) formulation of the Reynolds stresses is also tested. The turbulence compressibility corrections are often ignored and it is thought

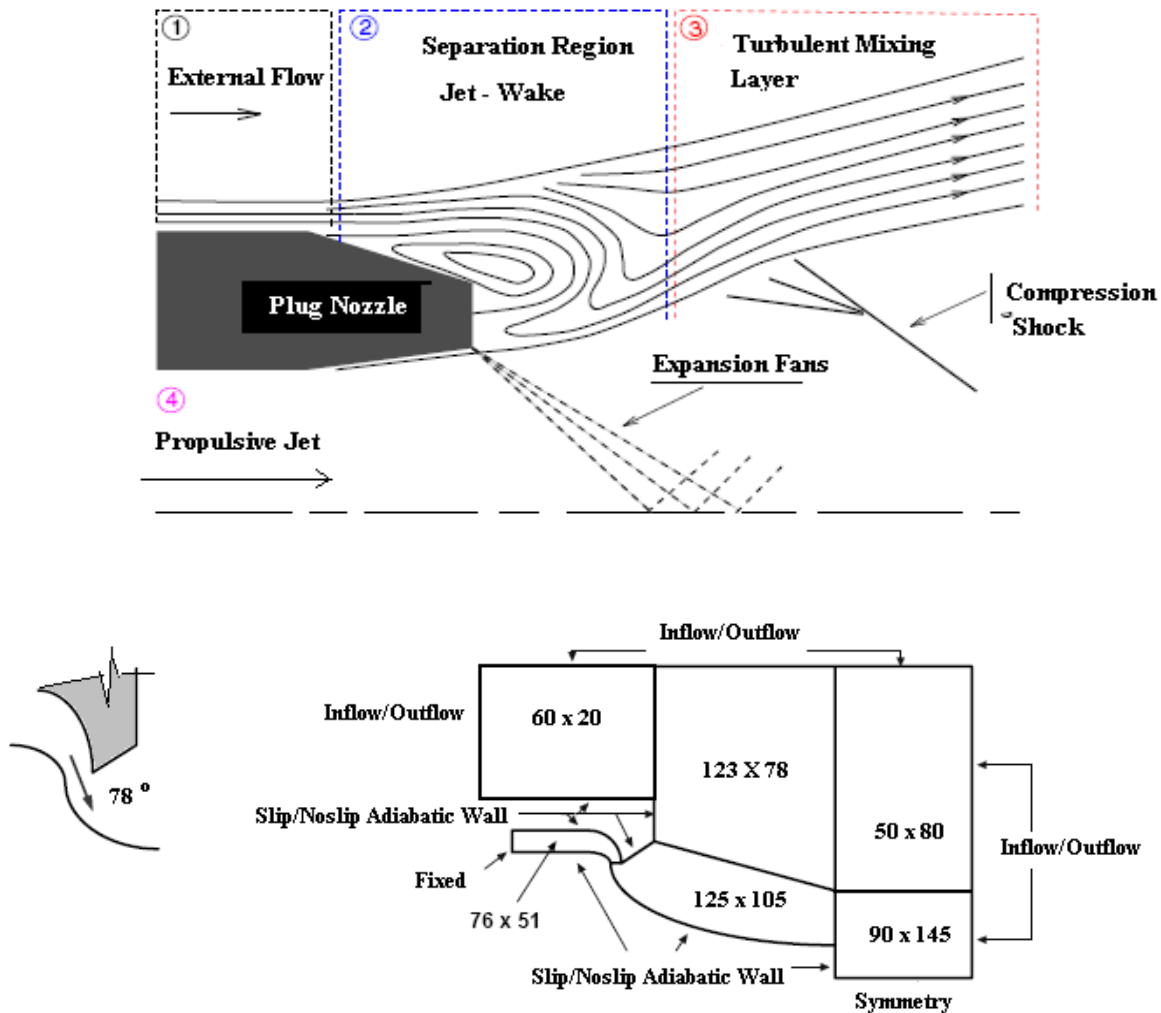


Figure 3 Schematic of Grid Block Structure and Boundary Conditions for Simulation of Aerospike Nozzle

that they play an important role in the complex flow that is created by the plug nozzle. Considering that the flow field is sensitive to the modeling of the two base flows (cylinder shoulder and plug base) and that the very high shearing rates create large turbulence kinetic energy levels, a correction based on the turbulent Mach number may seem inappropriate. To better understand how the turbulence corrections take place and how they

act on the flow field, the BSL case is selected and the source terms coefficients are studied. Recalling the formulation of the source term for the BSL model with compressibility correction from section 2, one gets the equation:

$$\zeta^* = \frac{3}{2}, M_{i0} = \frac{1}{4}, F(M_i) = (M_i^2 - M_i^0) \quad (12)$$

$$.H[M_i - M_{i0}]$$

$$\text{and } \beta^* = \beta_0^* \left[1 + \zeta^* F(M_t) \right] \quad (13)$$

$$\beta = \beta_0 - \beta_0^* \zeta^* F(M_t)$$

Therefore for the destruction term in the equation for the turbulence kinetic energy ($D_k = \rho k \beta^* \omega$) and for the turbulence dissipation rate ($D_\omega = \beta \rho \omega^2$) the two dissipation coefficients will change as the turbulence Mach number increases. In the turbulence kinetic energy equation the destruction will be increased, in the turbulence dissipation equation the opposite effect will take place. As a consequence, the eddy viscosity will decrease since it is defined as $\mu_t = \rho k / \omega$ and k is corrected to lower values while ω is corrected to higher values. Obviously the equations being coupled and being non-linear, only general trends can be given for these three quantities.

5. Result

The Figures 4 and 5 are showed for 8 turbulence models obtained by [1] and datas for author. For the case of a supersonic axisymmetric plug nozzle, the tests have been conducted by The Aeronautical Research Institute of Sweden (FFA). The plug nozzle is mounted in a cone-cylinder body which is held into the test chamber by a strut ; the plug nozzle chamber is fed by pressurized air which is sent through the strut. Wall pressures and velocity cross cuts using LDV have been performed by the FFA during the experimental runs. To investigate the performance of the various turbulence models introduced so far, the computations using the same flow conditions as recorded during the experiment (same plug nozzle chamber pressure) are used ; the walls are considered to be adiabatic. As the mesh size and the y^+ values are very small, one expects to obtain grid converged solutions. The plug wall pressures on the main body are shown for all 8 turbulence models [1] (see Figure 4 and 5). The agreement between [1] and the author with the experimental data is excellent except for the plateau region which is slightly over-estimated. The pressure plateau, or constant pressure

region, is located between the divergent and the location where the expansion fan at the lower shoulder base hits the wall. This results from the design chosen for the wall contour. All curves pass exactly at the pressure level recorded experimentally near the throat ;

the pressure levels near the end of the plug (before the base) are also very well predicted. It is interesting to note that all models give identical results regardless of the compressibility corrections and of the modeling of the Reynolds stresses. If one is interested in the wall surface pressure levels then a simple turbulence model gives excellent results. The next graph for the wall pressures on the plug shoulder and plug base is the Figure 5 for the wall pressures on the plug shoulder and plug base is examined next . This will be the basis for an in-depth discussion of the turbulence model as some large discrepancies are observed. There are two base flows ; the first large one is corresponding to the plug base for which half the plane is represented, the second smaller base flow is behind the plug lip which separates the outer free stream from the inner stream emanating from the plug nozzle chamber.

The characterization of the anisotropy nature of turbulence is done by inspecting the eddy viscosity tensor. We can write that the turbulent stresses are equal to the product of the following tensors :

$$\tau_{ij} = \mu_{ij} [S_{ij} - \delta_{ij} S_u] \quad (14)$$

where the deformation (strain) tensor has no trace. The μ_{ij} tensor is thus :

$$\mu_{ij} = \tau_{ij} [S_{ij} - \delta_{ij} S_u]^{-1} \quad (15)$$

The ratio of the Eigenvalues of the μ_{ij} matrix gives an indication of the anisotropy level (which is 1 for isotropic turbulence) : $|_{\max}|/|_{\min}|$. This ratio is presented in figure 6. Several important values can be spotted in specific zones indicating that the anisotropy effects are not negligible. This shows the usefulness of anisotropic turbulence models.

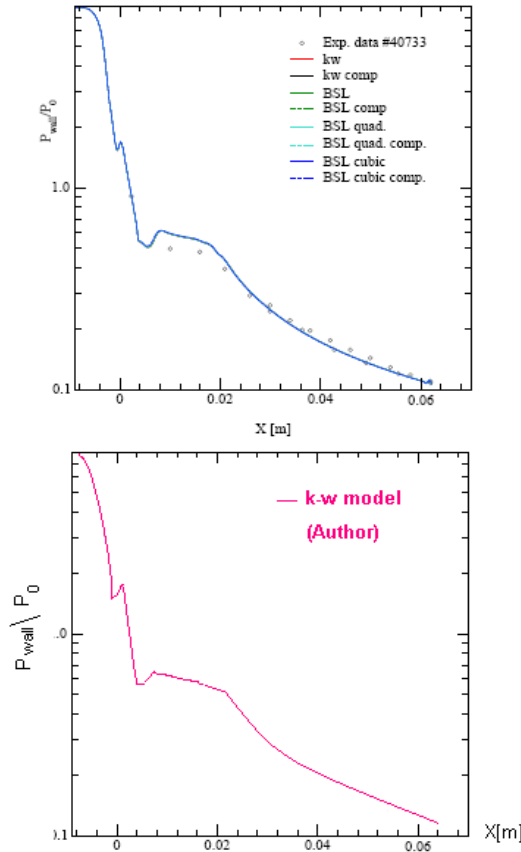


Fig. 4. – Wall Pressures on the Plug Body

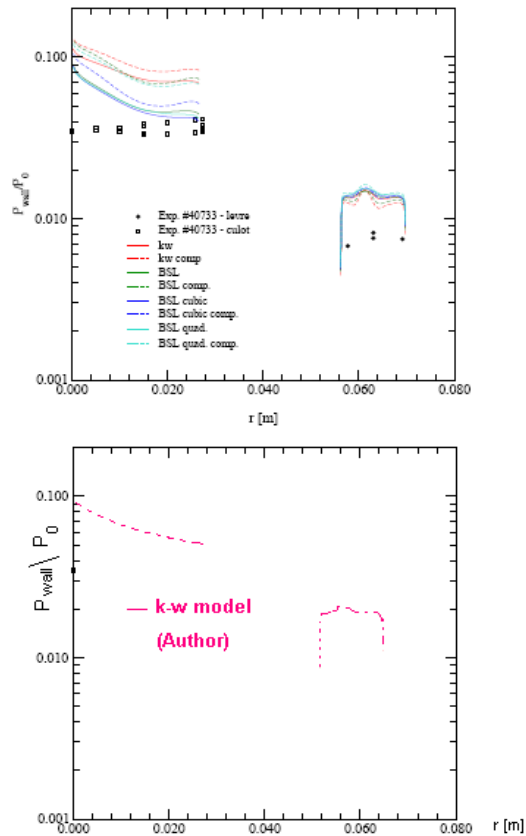


Figure 5 Wall Pressures on Lip the Plug Base

The velocity fluctuations in u are compared for the linear (Figure 6) and the non-linear model (Figure 7). It is possible to say that the values of u_0 obtained To summarize the last figures and the conclusions which have been made, the anisotropy level obtained with the cubic non-linear model as well as the nonequilibrium effects explain the difference observed in the wall pressures and the velocity profiles. One can wonder which one of these two effects is actually dominating the overall flow topology structure. The answer is that the non-equilibrium effects are the most important factor for such kind of complex flows. It is easy to imagine an extension of the multilayer (BSL) linear eddy viscosity model for compressible flows using only the non-equilibrium effects as described in the anisotropic models. This naturally leads to the SST model which almost corresponds to this description except that the

non-equilibrium effects are replaced by a simpler viscosity limiter.

6. Conclusion

The flow structure and the performance of the plug nozzle are numerically investigated. The afterbody flowfield is dominated by the behavior of the turbulent boundary layer. Thus the quality of CFD results depends strongly on the accuracy of the turbulence model. The afterbody configurations are often quite complex. Two turbulence models were investigated $k-\omega$ SST of Menter and $k-\epsilon$. The obtained results show that :

The boundary-layer separation on the boat-tail is correctly predicted with two models.

The basic characteristics of the flow field at the base region does not change whether the external flow is induced or not.

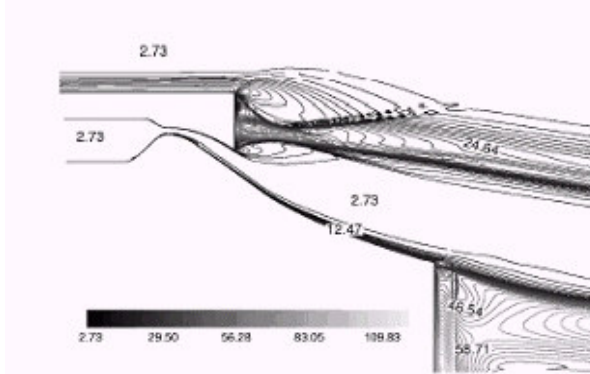


Figure 6 Flutuation of u for Linear BSL Model[1]

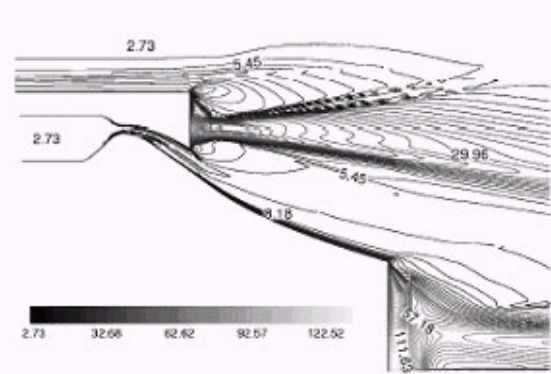


Figure 7 Flutuations of u for Cubic Model [1]

The base pressure is influenced by the ambient pressure when the pressure ratio is low and becomes independent from the ambient pressure when the pressure ratio is high. The base produces positive thrust when it is independent from the ambient pressure. Two high-pressure regions are observed along the nozzle axis. The shear layer impingement on the nozzle axis creates the first high-pressure region located near the nozzle surface. This high-pressure region becomes dominant when the pressure ratio is high. The envelope shock wave impingement on the nozzle axis creates the second high-pressure region located far distance from the base surface. This region becomes dominant when the pressure ratio is low. The reverse flow stagnates at the second high-pressure region when the pressure ratio is low. The external flow over the plug nozzle does not influence the pressure distributions over the plug surface for high-pressure ratios. The pressure thrust produced at the nozzle surface is not altered when the external flow is considered or not. The turbulence models validity has been explored for increasing flow complexity: wall attached flows (simple boundary layer), a mixing layer, The wall pressures are properly rebuilt for all models excepted for the pressure plateau corresponding to the re-circulation zone. Several attempts for improving the simulation in this region did not show any noticeable improvement. The results obtained for the two-dimensional and the axisymmetric cases are, from an overall point of view, good. However, important problems directly related to the turbulence properties have been highlighted.

7. References

- [1] Diedonné, W. Anisotropic Turbulence Modeling in Compressible Flow and Applications to Aerospice Plug Nozzles - Thesis of Docteur de L'universite de Poitiers -France, 2000.
- [2] Angelino, G. Theoretical and experimental investigation of the design and performance of a plug-type nozzle". VKI Technical Note 12, 1963.
- [3] Huang, D., Aerospice engine technology demonstration for space propulsion. Rocketdyne" / Rockwell International Corp. - AIAA paper No. 74-1080, 1974.
- [4] Launder, B., and Sharma, B., Application of the energy dissipation model of turbulence to the calculation of flow near a spinning disc". *International Journal of heat and mass transfer* 1, No. 2, 131-138, 1974.
- [5] Kolmogorov, A. Equations of turbulent motions of an incompressible fluid. *Izvestia Academy of Sciences, USSR; Physics* 6, 56-58, 1942.
- [6] Wilcox, D. C Reassessment of the scale determining equation for advanced turbulence models". *AIAA Journal* 26, No. 11, 1299-1310, 1988.
- [7] Menter, F. R., Two-equation eddy-viscosity turbulence models for engineering applications". *AIAA journal* 32, No. 8, 1994.

8. Copyright Statement

The author confirm that he, and their company, hold copyright on all of the original material included in their paper. They also confirm they have obtained permission, from the copyright holder of any third party material included in their paper, to publish it as part of their paper. The authors grant full permission for the publication and distribution of their paper as part of the ICAS2008 proceedings or as individual off-prints from the proceedings.